การประชุมวิชาการเครือข่ายวิศวกรรมเครื่องกลแห่งประเทศไทยครั้งที่ 18
18-20 ตุลาคม 2547 จังหวัด-ขอนแก่น

Design and Calibration of a Heliostat Prototype for Solar Energy Collections

Somchai Kiatgamolchai[1], Supavut Chantranuwathana[2], Manop Wongsaisuwan[3], Watanachai Smittakorn[4]
Chulalongkorn University
Bangkok, 10330, Thailand
Tel: 02-2186591 Fax: 02-2522889 E-mail: supavut.c@chula.ac.th

Abstract

A heliostat is a device that automatically tracks the sun as it moves across the sky and constantly reflects the sunlight to any desired location. In a large scale solar energy collection system, such as a central receiver system, heliostats are essential and cost 30 to 50 percents of the system's initial cost. This paper presents a first prototype of an on-going project of developing low-cost heliostats. The prototype has two independently rotating axes to orient the reflective mirror. Stepping motors driving worm gears are used to control these axes. The key idea to keep the cost down is to trade away accuracy but not repeatability. Repeatability allows accuracy to be recovered using an intelligent controller. This is done by estimating constant uncertainties affecting the accuracy of the system and using them to improve accuracy during actual operations. In this paper, positioning error of the heliostat in reflecting the sunlight to the target is assumed to be caused by the heliostat's installation error in orientation only. This is the dominating factor since a small orientation error can cause large error if the solar collector or the target is far away from the heliostat. This error is estimated by comparing the actual reflected lights on a screen and the desired locations using digital image processing. Two experimental results are presented. Although the results show somewhat improvement for targets inside the screen, the results are inconclusive that the proposed calibration and compensation techniques will improve accuracy.

1. Introduction

A heliostat is a device that automatically tracks the sun as it moves across the sky and constantly reflects the sunlight to a fixed location, typically a thermal collector. For a large scale solar collection system such as a central receiver system, heliostats are essential. In a central receive system, a number of heliostats are employed to reflect sunlight to a single central receiver. Total solar energy is directly proportional to the area of solar intake, the aperture of the system. Thus, the energy is related to the number of heliostats and their reflective area. Working temperature of the receiver, however, related to the system concentration ratio, the ratio of the receiver area to the aperture area. If flat reflective surfaces are used by the heliostats, this concentration ratio is directly proportional to the number of heliostats employed. To gain a high concentration ratio, a large number of heliostats are required or heliostats with curved reflective surfaces are required.

It is said that a field of tracking heliostats cost 30-50% of the total cost of a central receiver type of power plants [6, 8]. Therefore, lowering the cost of heliostats has been a main drive in solar energy research. In 1975, the United States Department of Energy (DOE) set a goal to produce heliostats at US$72 per square meters of reflective surface [6]. Using current technology, a rough estimate finds that a heliostat would cost around US$90-130 per m^2 with a reflective area around 160 m^2 per heliostat and at production levels of less than 2,500 per year. It is projected in [6] that the price can be reduced by 25% because of accumulated experience of the manufacturer after 100,000 units have been produced. On the other hand, new design such as the stretched-membrane type can cut cost 40% to about US$80 per m^2 with a 150 m^2 reflecting surface and at 2,500 unit per year [1]. This technology is still under development; e.g., at Sandia National Lab. in the US. It is important to note that the reduction in cost has been a result of a combination of improved design and increased reflective area. Increasing the size reduces the number of drive systems, pedestals, field wiring and control units. Newer designs have around 150-200 m^2 of reflecting surface.

[1] Department of Physics, Faculty of Science [2] Department of Mechanical Engineering, Faculty of Engineering. Corresponding author
[3] Department of Electrical Engineering, Faculty of Engineering [4] Department of Civil Engineering, Faculty of Engineering

Large heliostats are, however, expensive per piece. Hence, only a small number can be employed compared to using small heliostats. To get a high concentration ratio, these large heliostats must use curved reflective surfaces. Furthermore, the curvature of these reflective surfaces must be adjustable to avoid optical aberrations [7] which makes the focal point of the reflected light beam moved off the target as the sun move across the sky. It is approximated that, for a central receiver system with concentration ratio around 1,000, the accuracy of the heliostat system should be around 0.06 degree (3.5 arc min) [3] or less than 0.1 degree both in azimuth and altitude [2]. This suggests that large heliostats required stiff structure, powerful and accurate drive system due to weight of the system and wind loading. Instead of using adjustable stretched-membrane for a reflective surface, a number of small adjustable flat reflective surfaces mounted on the heliostat can also be used [4, 5].

Another approach is to use a large number of small heliostats. The large number of heliostats ensures high concentration ratio without requiring curved reflective surfaces. This approach is, however, not taken seriously earlier since each heliostat required a drive system and associated electronics. As a result, their cost can become the main cost of the system which should be the cost of the reflective surfaces. However, recent development in electronic devices in the last few decades makes this approach more attractive. Furthermore, the smaller size may reduce the structural cost and the larger number may allow each heliostat to be less accurate. This is the approach taken by the authors' solar research group. This paper presents an on-going development in designing low-cost heliostats by the authors.

In order to reduce the cost of heliostat, high accuracy drive system and high precision structural manufacturing cannot be used. For example, open-loop drives are typical for heliostats. A method is to sacrifice accuracy to save cost but retain repeatability as much as possible. In this way, accuracy can still be recovered using intelligent electronics with calibration and compensation techniques. Due to a large number of heliostats, calibration and compensation must be done automatically to reduce installation and maintenance costs. This paper concentrated on this calibration and compensation techniques.

In a paper by Baheti et al [2], a method to improve accuracy by implementing calibration and compensation was proposed. This technique uses the sun's position from a sun sensor mounted on the reflective surface of a heliostat as a reference to calibrate for the heliostat's deterministic positioning error in the drive and the orientation of the heliostat. In calibration mode, the heliostat is pointed to the sun using the sun sensor and a positioning servo system. This actual sun's position will not be the same one calculated by the heliostat because of error in the drive and orientation. This difference, when collected in number, can be used to estimate the errors. The errors are then used to improve the heliostat's accuracy in normal operations. Significant improvements were observed.

For a heliostat field with a large number of heliostats, this technique may not be practical. The sun sensor must be relocated from a heliostat to another manually and a good calibration required a long period of time (5 hours [2]). This paper proposed a method using a stationary digital camera and a stationary target screen. In calibration mode, a heliostat is commanded to reflect the sunlight to the middle of the screen. Actual location of the sunlight will not be in the middle, however, because of the error in the heliostat's drive, the error in manufacturing and the error in installation. The location of the actual sunlight, when measured in number, can be used to estimate the errors. These errors are used by the heliostat during its normal operations to improve its accuracy. Although, calibration data are required to be taken during a long period of time, they can be taken in intervals. Hence, a number of heliostats can be calibrated during the same period of time. For example, if data have to be taken at an interval of 5 minutes and each point of data uses 30 seconds, then as much as 10 heliostats can be calibrated at the same time.

The rest of the paper is organized as follows. In section 2, the hardware design of the heliostat prototype is described. In section 3, the calibration and compensation methods are described. In section 4, experimental results are presented. Finally, summary and conclusion are presented in section 5.

2. Hardware Design

A basic working principle of a heliostat is shown in Fig. 1. In general, the unit vector $\hat{t}$ pointed to the target is a constant but varies with the location of the heliostat relative to the target. The unit vector $\hat{s}$ pointed to the sun varies continuously but stays approximately in a plane each day. To reflect the sunlight to the target, a heliostat must be able to control the normal vector, $\hat{n}$, of its reflective surface so that $\theta_1=\theta_2$. Knowing $\hat{t}$ and $\hat{s}$, the vector $\hat{n}$ can be easily computed as

$$\hat{n} = (\hat{t} + \hat{s}) / |\hat{t} + \hat{s}| \quad (1)$$

In this work, azimuth-altitude drives shown in Fig. 2 are used to orient the reflective surface. These two axes can be driven independently to orient the mirror. To simplify the calibration and compensation process, the azimuth axis and the altitude axis are designed to intersect at the middle of the reflective surface. This

ensures that the middle point of the reflective surface remains fixed for any rotation of the driving axes.

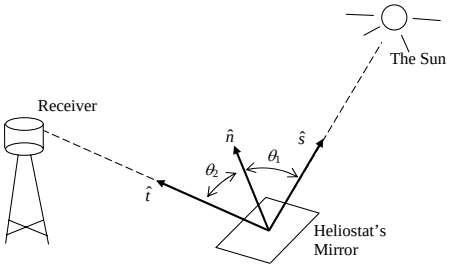

Figure 1. Basic principle of heliostat

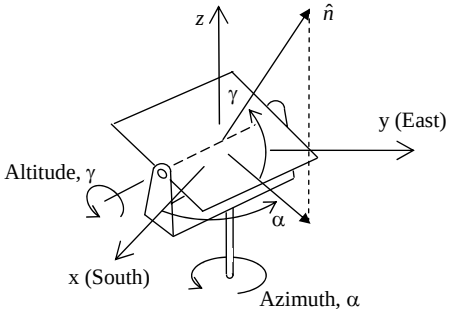

Figure 2. Orientation of heliostat

Stepper motors are used to drive azimuth and altitude axes. Stepper motors are inexpensive compared to servo motors while allowing some positioning capability. A pulse command signal can be sent to the motor to turn the motor one step (a constant angular displacement). However, a stepper motor does not have a position sensor and care must be taken to make sure that each step is completed as commanded to ensure that the correct angular position of the motor can be deduced from the number of pulses of the command signal. Furthermore, a stepper only has a small amount of holding torque when its windings are not energized. So, a worm gear mechanism is chosen for its self-locking feature. Self-locking allows the heliostat to keep its reflecting surface still under wind loading without constantly losing energy to its driving motors.

In this work, a heliostat prototype was made using a single-stage 100 to 1 worm gear with a 200 step per revolution stepper motor for each of the two axes. Fig. 3 shows a picture of the prototype. This prototype was designed for a reflective surface of 20 x 30 cm^2. The resolution is 0.018° for each of the driving axes with 0.185° backlash for the azimuth axis and 0.111° for the altitude axis. These backlashes are significant comparing to the resolution but can be compensated by spring loadings. Nonetheless, they do not effect the results in this paper since error of the heliostat in reflecting the sunlight are significantly larger.

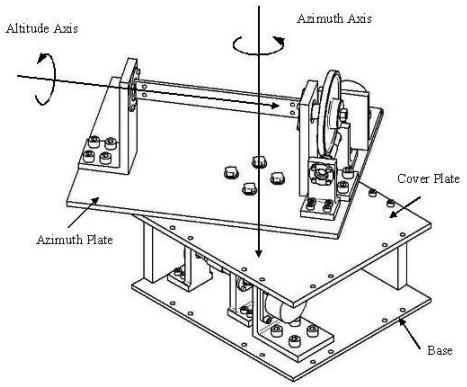

Figure 3. The Heliostat prototype

3. Software Design

Two reference frames were used in the calibration of the heliostat, namely "mirror" and "sun-earth" frames. Both frames have their origin at the center of the mirror. The mirror frame is attached to the heliostat with the azimuth axis as the z-axis. Ideally, the x-axis and the y-axis should be pointed to the south and east direction respectively with the x-y plane perfectly leveled. The sun-earth frame is the reference frame in which the sun position and the target vector are calculated. Its horizontal plane is parallel to the earth surface. The +x axis is in the south direction and the +y axis is in the east direction. Ideally, these two frames must be identical so that the mirror, controlled relative to its frame, can reflect the sunlight to a target point. In general, difference can still exist even with careful installation. In this work, we assume that these two frames share the same origin but are rotationally different by a set of Euler's angles. Knowing the Euler's angles, one can transform any vector from the mirror frame to the sun-earth frame, and vice versa. Obviously, there are other factors that affect the accuracy of a heliostat, but, in this work, only this orientation error is considered.

Let the center of mirror be a point O, given the vector $\hat{t}$ and $\hat{s}$ measured in the sun-earth frame, the mirror's normal vector can be calculated as shown in Eq. (1). This vector will be called $\hat{n}_C$. This vector is then used to calculate the azimuth and the altitude angle of the heliostat driving axes. These angles are, however, measured relative to the mirror frame. Since the mirror frame are not identical to the sun-earth frame, the actual mirror's normal vector, $\hat{n}_A$, will not be identical to the desired vector. This will cause the actual target vector, $\hat{t}_A$, to move off the desired target. Using the Euler's angles, we can relate

$$\hat{n}_C = R\hat{n}_A \tag{2}$$

where $R \in \Re^{3x3}$ is a constant rotational matrix. Suppose *n* pairs of ($\hat{n}_C, \hat{n}_A$) are measured, an estimate of R can be obtained using the standard Least-square technique as

$$R_e = (S'S^T)(SS^T)^{-1} \quad (3)$$

where $S' \in \Re^{3xn}$ is a matrix of the measured $\hat{n}_C$ vectors and $S \in \Re^{3xn}$ is a matrix of the measured $\hat{n}_A$ vectors.

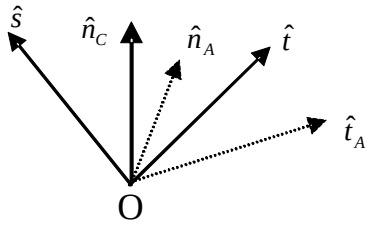

Figure 4. Vectors for calibration

For each $\hat{n}_C$, $\hat{n}_A$ can be calculated from the vectors $\hat{t}_A$ and $\hat{s}$. The sun vector is assumed to be precisely known. The calculation of the actual target vector is achieved by using a flat screen as the target. A digital camera was used to take a picture of the reflected sunlight on the screen and calculate the vector $\hat{t}_A$. A digital camera was installed such that the center of screen appears approximately at the center of the picture and the camera optical axis is approximately perpendicular to the screen. With this configuration, it is possible to map a point on the screen to a pixel on the picture and vice versa. Consider the image (point P) in Fig. 5, where points A, C, and D are the screen corners. Let (x, y, z) be the sun-earth coordinate and (i, j) be the pixel coordinate. The position of point P appears on the screen can be calculated using a relation

$$\vec{P} - \vec{C} = M\hat{u} + H\hat{z} \quad (4)$$

where $\hat{u}$ is a directional vector from point C to D and $\hat{z}$ is a directional vector from point C to A. Normally the position C and D are at the same height from the earth surface, therefore M is a distance between point C and P on the x-y plane,

$$M = \frac{i_P - i_C}{i_D - i_C}\sqrt{(x_D - x_C)^2 + (y_D - y_C)^2} \quad (5)$$

Also, since points A and C have the same (x, y) coordinate, H can be calculated in the same manner as

$$H = \frac{j_P - j_C}{j_A - j_C}(z_A - z_C) \quad (6)$$

The pixel-coordinate of the mirror image could be quite difficult to calculate because the image boundary is not clearly seen. In this work, the coordinate is obtained using a centroid calculation. Each pixel is represented by red, green and blue values from 0 to 255.

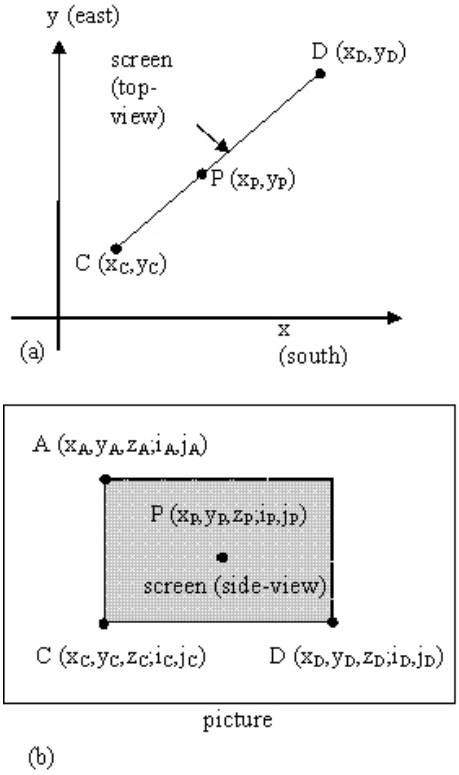

Figure 5. The calibration screen as seen from top-view and side view, (a) the coordinates of two bottom screen corners and (b) the picture of screen as to be taken by a camera

We define "brightness" (I) from the sum of these values. The centroid (i_p, j_p) can be calculated with

$$i_P = \frac{\sum_{i,j} I_{ij} i}{\sum_{i,j} I_{ij}}, \quad j_P = \frac{\sum_{i,j} I_{ij} j}{\sum_{i,j} I_{ij}} \quad (7)$$

This has to be summed for all pixels that are part of the reflected sunlight. To speed up the calculation process, we set a criterion that any pixel with intensity less than the average pixel-intensity of the whole picture by six times the standard deviation can be considered out of the image area. The calibration procedure is as follows.

1. Obtain the position of the mirror and the screen coordinate.

2. Manually control the heliostat to reflect the sunlight onto the screen. Take a photograph, calculate the position of the image, and hence calculate the initial normal vector of the mirror.
3. Command the heliostat for the first target point by adjusting the normal vector of the mirror.
4. Take a photograph and calculate the actual normal vector.
5. Repeat the last two steps for other target points.
6. Calculate the rotational matrix.

The tracking procedure is as follows.

1. Calculate the actual normal vector and then apply the rotational matrix to yield the "command" normal vector.
2. Move the heliostat according to the "command" normal vector.

4. Experimental Results

The heliostat was tested on clear days using a building wall as a calibration screen. The size of the screen is 2x2 m^2 and it is 13 cm above the floor. The heliostat was placed on the floor at 10 m from the screen. Fifteen target points inside the screen area are used for calculating the rotation matrix. The calibration took approximately 3 minutes. Several target points on the wall, inside and outside the calibrated screen were selected to test the accuracy in controlling the heliostat. Two test results are presented.

Fig. 6-8 show results taken on Jan 17th 2004. Fig. 6 shows the position of target points and the reflected sunlight image on the wall using non-calibrated and calibrated methods. To estimate the degree of off-target, the azimuth and altitude angles of each point were calculated. For the azimuth angle, the mirror-screen line was taken as a reference (zero azimuth). Fig. 7 shows the azimuth error angles, the difference in azimuth angles between the target and the actual locations, versus azimuth angle of the targets (relative to the reference). It can be seen that the accuracy of the calibrated method is generally better within the area shown. The y-interception point of the calibrated data yields a smaller value of 0.026 which indicates that it gives less error within the calibrated screen. However, the calibrated method gives higher slope which means that the error will be greater magnified at higher relative azimuth angle. For the altitude error angles, as seen in Fig. 8, it was found that the calibrated results gives smaller values in the y-interception point which indicates that it can control the direction of the reflected sunlight better within the calibration screen. The slopes are, however, similar.

Fig. 9-10 show results taken on Jan 20th 2004. Fig. 9 shows that the errors in azimuth angles are generally comparable for the range of data shown. The calibrated method shows better accuracy inside the screen but generally worse as the target move farther from the screen because of the higher slope. Fig. 10 shows the calibrated method is generally more accurate for the range of data shown. Although it has smaller slope, it has higher y-interception point.

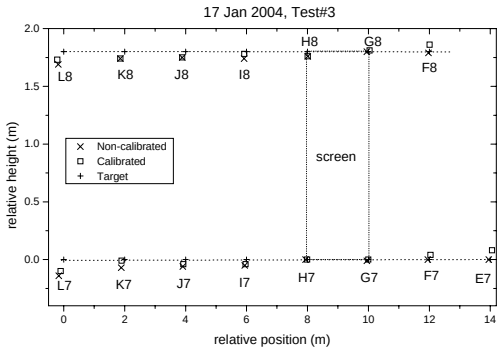

Figure 6. The position of target points and the reflected sunlight on the wall using non-calibrated and calibrated methods. (The picture is not drawn to scale)

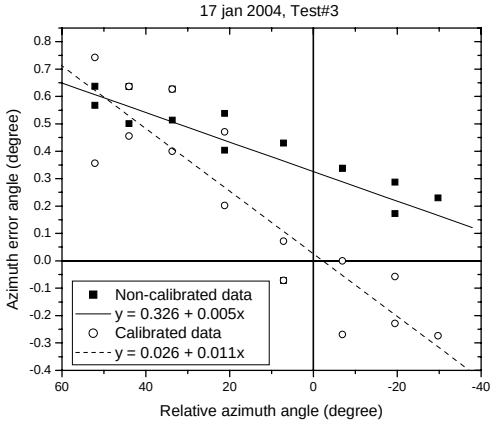

Figure 7. Azimuth error angle from non-calibrated and calibrated methods (Jan 17th 2004)

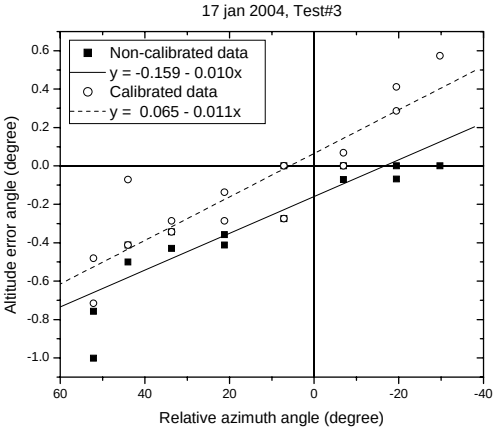

Figure 8. Altitude error angle versus the relative azimuth angle (Jan 17th 2004)

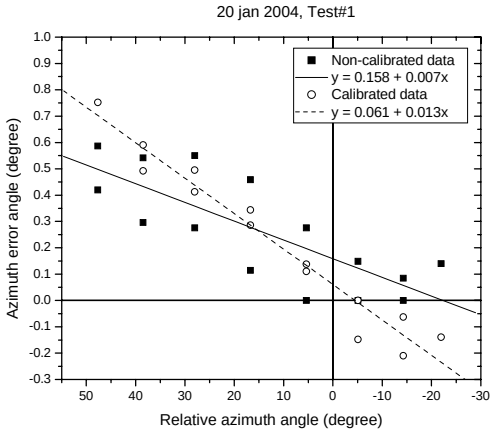

Figure 9. Azimuth error angle from non-calibrated and calibrated methods (Jan 20th 2004)

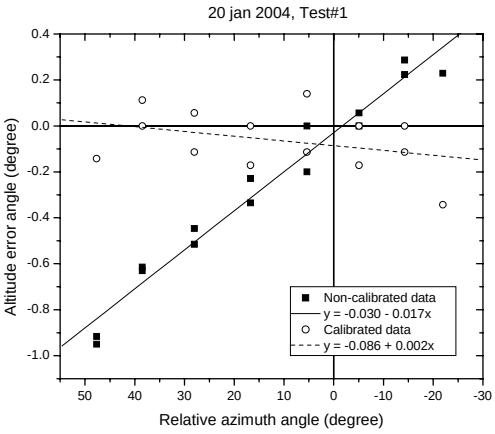

Figure 10. Altitude error angle versus the relative azimuth angle (Jan 20th 2004)

For the two results, they seem to show that accuracy is significantly improved in either one of the two angles while slightly reduced in the other. It is not conclusive, however, that the calibration method is more accurate, hence more testing is required; for example, with longer period of time during the calibration or with a bigger target screen. Since, the actual target and the calibration screen will not likely be in the same location, the ability to obtain accurate results outside the screen is essential. Furthermore, it is remained to be determined if the current error compensation scheme has enough flexibility to compensate for all the major causes of errors.

5. Summary and Conclusion

In this paper, a design of a heliostat prototype is presented. The key design objective is to reduce cost of the heliostat by using intelligent calibration and compensation techniques to obtain the necessary accuracy. Calibration and compensation methods based on the image processing of the reflected sunlight have been proposed and tested. Only the error in orientation of the heliostat is considered in this work. The test results show that the error within the calibrated screen is generally reduced. However, the results are inconclusive that the calibration will improve the accuracy.

6. Acknowledgement

We would like to thank Dr. Viroj Tantraporn for his guidance throughout this project and we would like to thank the Department of Alternative Energy Development and Efficiency for its financial support and permission to publish this paper.

References

[1] Alpert, D.J., Houser, R.M., Hackes, A.A., Erdman, W.W., ``The Development of Stretched-membrane Heliostats in the United States,'' Solar Energy Materials, 21, 1990, pp.131-150.

[2] Baheti, R.S., Scott, P.F., ``Design of Self-Calibrating Controller for Heliostats in a Solar Power Plant,'' IEEE Transaction on Automatic Control, Vol. AC-25, No. 6, Dec. 1980.

[3] Blanco-Meriel, M., Alarcon-Padilla, D.C., Lopez-Moratalla, T., Lara-Coira, M. ``Computing the Solar Vector,'' Solar Energy, Vol.70, No.5, pp.431-441, 2001.

[4] Chen, Y.T., Bligh, T.P., Chen, L.C., Yunus, J., Kannan, K.S., Lim, B.H., Lim, C.S., Alias, M.A., Bidin, N., Aliman, O., Salehan, S., Rezan, S.A., TAM, C.M., Tan, K.K., ``Non-imaging, Focusing Heliostat,'' Solar Energy, V. 71, No. 3, 2001, pp.155-164.

[5] Chen, Y.T., Chong, K.K., Lim, C.S., Tan, K.K., Aliman, O., Bligh, T.P., Tan, B.K., Ismail, G., ``Report of the first Prototype of Non-imaging Focusing Heliostat and Its Application in High Temperature Solar Furnace,'' Solar Energy, Vol. 72, No. 6., 2002, pp.551-544.

[6] Krawiec, F., ``Concepts of Learning and Experience in Developing Solar Thermal Technologies,'' Technological Forecasting and Social Change, 24, 1983, pp.207-246

[7] Meinel, A.B., Meinel, M.P., Applied Solar Energy, An Introduction, Addison-Wesley Publishing Company, 1977

[8] Zavoico, A.B., Gould, W.R., Kelly, B.D., Pastoril, I.G., ``Solar Power Tower (SPT) Design Innovations To Improve Reliability and Performance - Reducing Technical Risk and Cost,'' Proceedings of Solar Forum 2001, Solar Energy: The Power to Choose, April 21-25, 2001, Washington, DC.